Enhancement of Flow Boiling CHF on a Downward-facing Heated Wall using a Hydrophilic Metallic Wire-mesh

In Yeop Kang[a], Hyungdae Kim[a*]
[a] *Department of Nuclear Engineering, Kyung Hee University, Yong In, Republic of Korea*
E-mail: hdkims@khu.ac.kr

***Keywords : Flow boiling, Critical heat flux, Heat transfer coefficient, Dry area fraction**

1. Introduction

The IVR (in-vessel corium retention)-ERVC (external reactor vessel cooling) strategy is an effective approach for maintaining reactor vessel integrity during severe accidents in nuclear power plants [1]. Since the Fukushima accident in 2011, interest in IVR-ERVC has increased substantially. The performance of IVR-ERVC is strongly influenced by nucleate boiling on the reactor vessel lower head. When the decay heat generated within the vessel is sufficiently high, a critical heat flux (CHF) condition may occur on the downward-facing heated surface of the lower head, potentially threatening vessel integrity. Accordingly, CHF enhancement techniques applicable to downward-facing boiling surfaces are required to improve the cooling capability of ERVC systems.

To demonstrate the feasibility of IVR-ERVC, numerous experimental and analytical studies have been conducted [2-5]. One study investigated various CHF enhancement approaches have been investigated, including nanofluids, surface modification, micro-/mini-channel structures [6]. These methods can enhance CHF under downward-facing conditions. However, they involve practical challenges in long-term operation, maintenance, and large-scale implementation.

Kim et al. [7] proposed stainless-steel hydrophilic wire-mesh structures to enhance CHF in pool boiling without altering the physical or chemical properties of the base boiling surface. Their results suggested that a wire-mesh suppresses the formation and growth of dry spots by promoting capillary liquid replenishment along hydrophilic wires.

Compared with alternative enhancement methods, the wire-mesh approach is mechanically simple and is potentially scalable for large-area implementation while minimally affecting bulk fluid properties. In the present study, the CHF enhancement performance of a hydrophilic wire-mesh layer for ERVC application is experimentally evaluated under flow boiling on a downward-facing heated wall. To investigate the underlying mechanisms, bubble dynamics and liquid-vapor phase distribution near the boiling surface are visualized using high-speed video(HSV) and infrared (IR) thermography.

2. Experimental methods

2.1.Flow boiling facility and instrumentation

Figure 1 shows the flow boiling facility used in this study. The loop consisted of a rectangular channel (test section), a storage tank, a preheater (15 kW), a centrifugal pump (Hydra-Cell G10X), and a heat exchanger (22 kW). Deionized water was used as the working fluid. To perform inclination tests, a tiltable optical table was used to set and maintain the prescribed inclination angles of the test section.

Boiling behavior was visualized using an infrared camera and a high-speed camera. The IR images were recorded at 500 fps, while the HSV images were recorded at 5,000 fps.

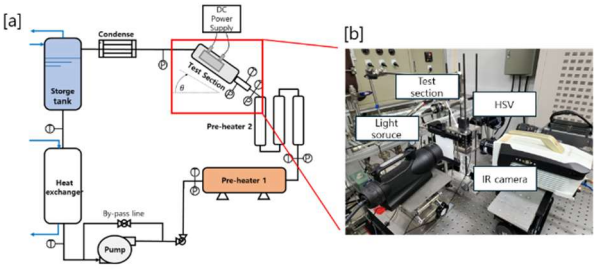

Figure 1. (a) Schematic illustration of test facility, (b) test section set up using IR and HSV

2.2. Experimental conditions

Based on a previous study [8], the coolant mass flow rate under IVR-ERVC conditions was estimated to be 1,200 kg/s. Accordingly, the mass flux in the present experiments was fixed at 200 kg/m^{2}s, corresponding to the value estimated for the target conditions. The inlet subcooling was maintained at 5 K and all tests were conducted at atmospheric pressure. The inclination angle was varied as 15°, 30°, 45°, 60°, and 90°. The experimental uncertainty in the applied heat flux was 8.8%.

2.3.Electrochemical etching of wire-mesh

Figure 2 summarizes the electrochemical etching procedure used to create hydrophilic microstructures on stainless steel 304 wire-mesh (12×45 mm^2, wire diameter 0.5 mm, opening length 1.31 mm). The mesh was etched in an aqua regia solution while the solution was stirred to maintain uniformity and then rinsed with deionized water and fully dried prior to the boiling tests [7]. Notably, the etched mesh exhibited hydrophobic

behavior in the dry state but transitioned to hydrophilic behavior once wetted.

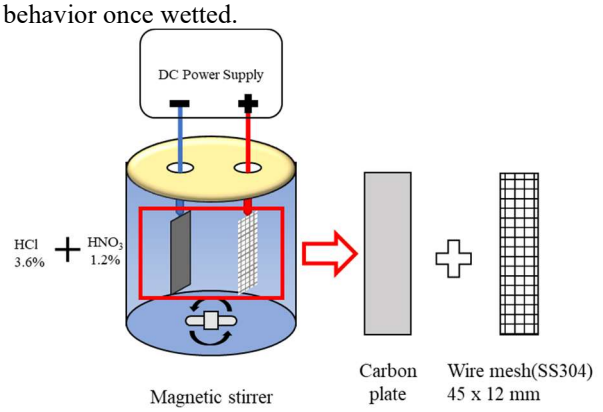

Figure 2. Electrochemical etching process of a wire-mesh sample to fabricate hydrophilic properties

2.4. Experiment boiling surface process

Figure 3 shows the silicon wafer heater sample preparation used in the test section. A 500 μm thick silicon wafer was employed as the heater substrate. A 2 μm thick silicon dioxide (SiO_2) layer was thermally grown on the boiling surface to provide electrical insulation from the working fluid. On the backsides of the wafer, 100 μm thick Au film and 10 μm thick Ti film were deposited to form an electrical connection between the heater and the DC power supply.

Because the silicon wafer is partially transparent in the IR spectral band (λ = 3-5 μm), four carbon graphite black dots were coated on the backsides of the substrate to obtain an average surface temperature. After etching, the wire-mesh was bonded onto the bare silicon wafer specimen using epoxy.

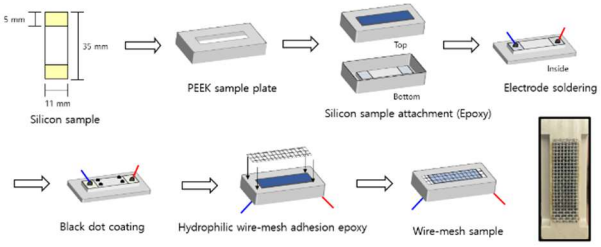

Figure 3. Preparation of wire-mesh boiling samples

3. Results and discussion

3.1. Boiling curve and heat transfer coefficient

Figures 4 and 5 present the boiling curve and the corresponding heat transfer coefficients (HTC), respectively. The experimental results indicate that the CHF increased with increasing inclination angle for both the bare surface and the wire-mesh surface. For the wire-mesh surface, the CHF was enhanced by approximately 33–50% compared with the bare surface. In addition, the HTC for the wire-mesh surface was improved by more than 50% relative to the bare surface.

These trends suggest that boiling heat transfer becomes more effective as the inclination angle increases. As the inclination increases, buoyancy effects become stronger, influencing bubble departure and coalescence and ultimately affecting the development of slug bubble flow [9]. Regarding the HTC behavior, with increasing heat flux (and the accompanying rise in wall temperature), the bare surface exhibited only a marginal increase or even a decrease in HTC as, whereas the wire-mesh surface maintained a comparatively high HTC.

In addition, at relatively low wall superheat (low heat flux) conditions, portions of the wire-mesh cases exhibited an HTC lower than that of the bare surface. This behavior is attributed to the wire-mesh grid geometry, which can hinder bubble departure under low heat flux conditions, causing bubbles to become temporarily trapped within the mesh grid and thereby reducing effective heat transfer. These observations are consistent with the HSV and IR visualization results presented in Sections 3.2 and 3.3. In those sections, bubble dynamics and liquid–vapor phase behavior were analyzed under low and high heat flux conditions at inclination angles of 15° and 60°, respectively.

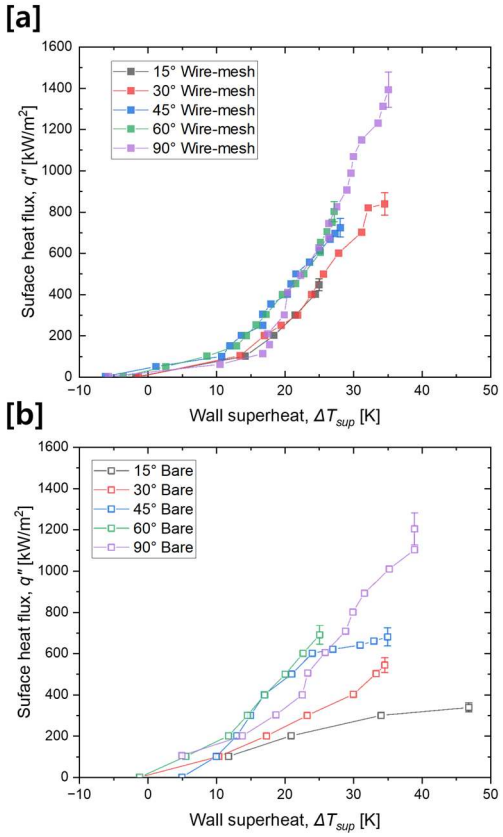

Figure 4. Boiling curve: (a) the wire-mesh case , (b) bare case

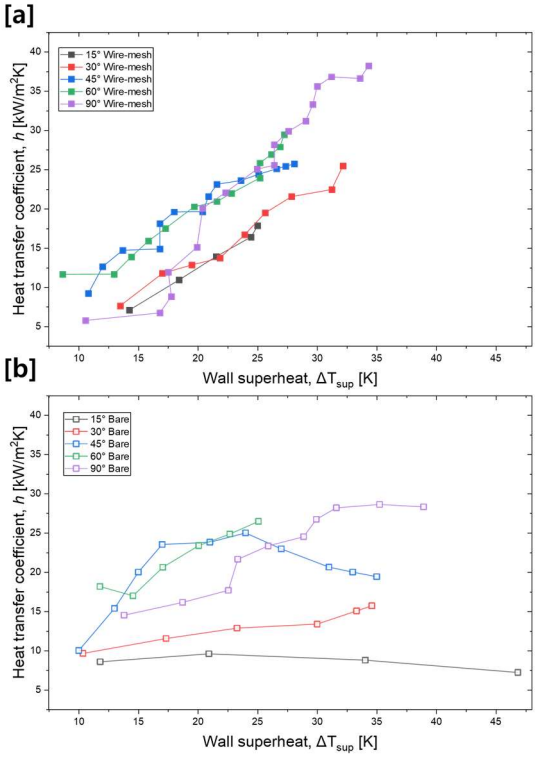

Figure 5. Heat transfer coefficient: (a) the wire-mesh and (b) bare case

3.2. Bubble dynamics

Figures 6 and 7 compare bubble dynamics on the wire-mesh and bare surfaces under low and high heat flux conditions. The low heat flux case (Fig. 6) was obtained at an inclination angle of 60° with a heat flux of 200 kW/m². For the high heat flux condition (Fig. 7), typical cases are shown at 90% of CHF for 15° and 95% of CHF for 60°.

Under the low heat flux condition, the bare surface exhibited frequent bubble coalescence and bubble sliding driven by the surrounding liquid flow. In contrast, on the wire-mesh surface, bubbles were observed to be temporarily trapped by the mesh grid immediately after nucleation, which delayed coalescence compared with the bare surface. After growing to a certain size and merging, the bubbles on the wire-mesh surface subsequently exhibited sliding along the heated wall.

In the high heat flux images shown in Figures 7, slug bubbles moving along the heated wall were observed for both surfaces. The color-highlighted slug bubbles are noticeably longer on the bare surface, whereas they form with a relatively shorter length on the wire-mesh surface, presumably due to the presence of the mesh grid. Equation (1) provides a CHF correlation for flow boiling conditions [10], in which CHF is assumed to occur when the liquid film beneath a slug bubble dries out. According to Eq. (1), a shorter slug bubble length leads to a higher CHF. Therefore, the reduced slug-bubble length observed in Fig. 7 is expected to contribute to the CHF enhancement.

$$q''_{CHF} = a_1 \frac{\rho_l \delta_m (h_{fg} + a_2 \Delta h_{sub})}{l} u_g \quad (1)$$

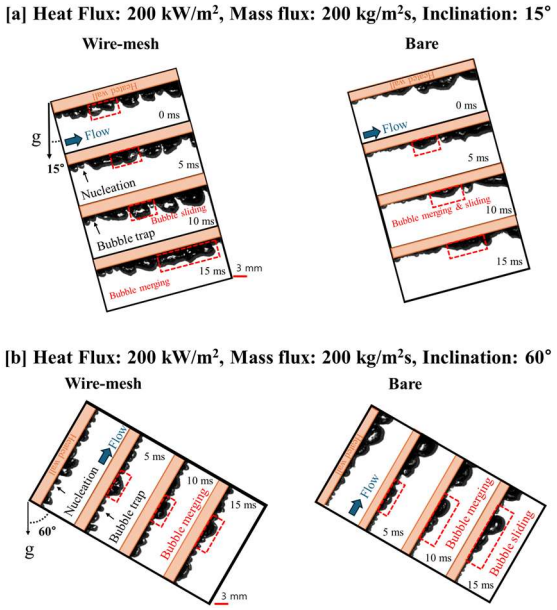

Figure 6. Bubble dynamics on the bare and wire-mesh cases under low heat flux conditions: (a) inclination 15°, (b) inclination 60°

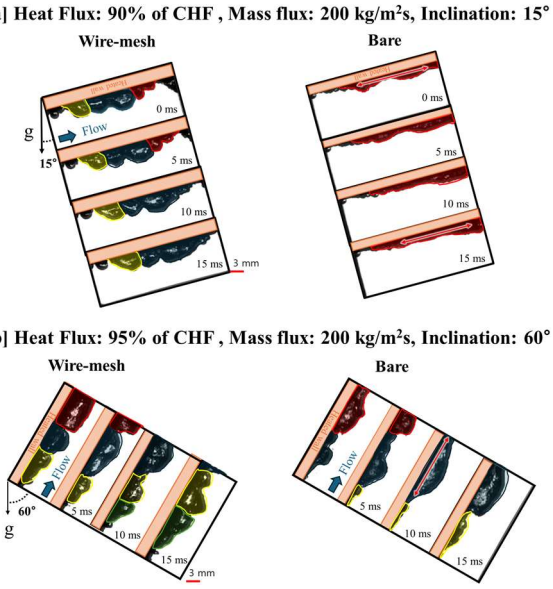

Figure 7. Bubble dynamics on the bare and wire-mesh cases under high heat flux conditions: (a) inclination 15°, (b) inclination 60°

3.3. Liquid-vapor phase distribution

Figure 8 presents IR images of the near-wall flow behavior on the hydrophilic wire-mesh surface at inclination angles of 15° and 60° under a heat flux of 200 kW/m². Bubble nucleation on the heated wall and subsequent coalescence were observed. During the coalescence process, the hydrophilic wire mesh promoted capillary-driven liquid wicking toward the

vicinity of the merged bubbles, which is consistent with the behavior reported in previous studies [7, 11].

To quantify the phase distribution, the time evolution of the liquid–vapor distribution was evaluated as shown in Figure 9 for a representative case at an inclination angle of 60° and a heat flux of approximately 95% of CHF. The liquid–vapor phase distribution was obtained using MATLAB (R2025b) by binarizing the IR images and calculating the corresponding liquid and vapor area fractions. For the bare surface, the vapor fraction ranged from 30% to 50%, whereas for the wire-mesh surface it remained lower, at approximately 20% to 30%. This reduced vapor fraction in contact with the heated wall indicates that capillary pumping through the wire-mesh continuously supplies bulk liquid to the heated wall, thereby suppressing the lateral expansion of dry spots.

Based on these observations, Figure 10 summarizes the liquid–vapor phase fractions for all test conditions. For the bare surface, the vapor fraction prior to CHF was typically around 40%, while the wire-mesh surface exhibited a lower vapor fraction of approximately 22–30%. These results support that suppression of dry spots expansion via capillary pumping is a primary mechanism responsible for CHF enhancement on the hydrophilic wire-mesh surface.

This mechanism is particularly relevant at high heat flux conditions, where bubble coalescence can promote the formation and growth of dry regions. Because the heat transfer coefficient in vapor covered areas is lower than that in liquid covered or thin film regions, the formation of a dry region can induce local overheating and ultimately lead to CHF. Therefore, increasing liquid supply to the heated wall via capillary pumping through a hydrophilic wire mesh is expected to suppress dry region expansion, thereby delaying the onset of CHF.

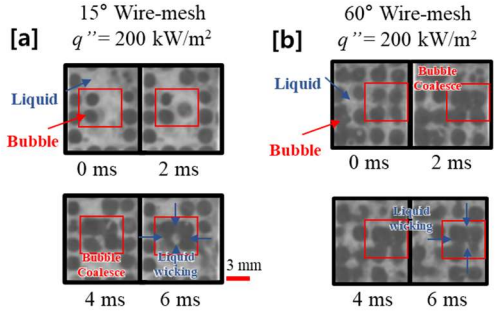

Figure 8. Bubble behavior on the wire-mesh cases at the heated wall: (a) inclination 15°, (b) inclination 60°

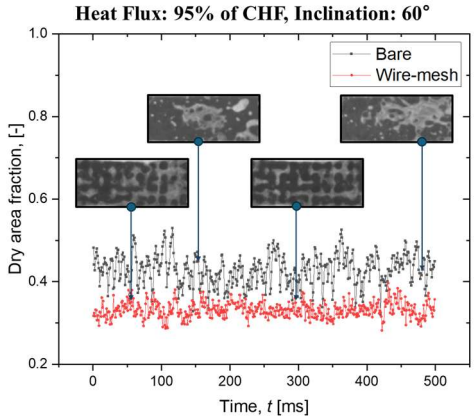

Figure 9. Dry area fraction at heat flux 95% CHF, and an inclination angle of 60°

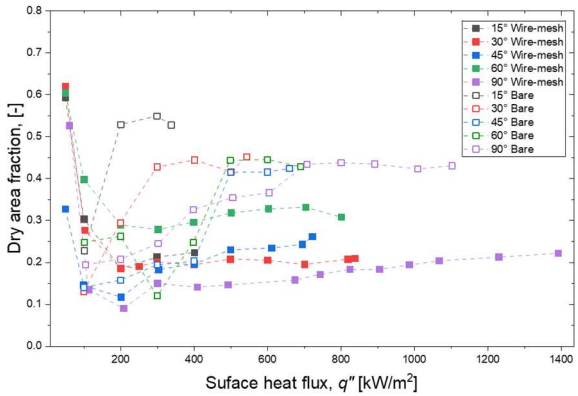

Figure 10. Dry area fraction as a function of heat flux for all test conditions

4. Conclusions

This study experimentally investigated flow boiling heat transfer and CHF on a downward-facing heated wall using a hydrophilic metallic wire mesh for IVR–ERVC relevant conditions. Experiments were conducted at atmospheric pressure with deionized water at a mass flux of 200 kg/m²s, an inlet subcooling of 5 K, and inclination angles of 15°–90°. Compared with the bare surface, the wire-mesh surface increased CHF by approximately 33–50% and improved the HTC by more than 50% over a wide range of conditions.

To analyze the CHF enhancement mechanism of the hydrophilic wire mesh, HSV and IR measurements were employed. The IR visualization observations suggest that the hydrophilic mesh promotes capillary-driven liquid replenishment toward the heated surface, enabling cooling liquid to flow around the dry spot region and hindering its lateral expansion. It also influences slug bubble dynamics. This observation is consistent with the liquid–vapor phase analysis, where the bare surface typically showed a vapor fraction of ~40% prior to CHF, while the wire-mesh surface maintained a lower vapor fraction of 22–30%. Overall, capillary pumping through the hydrophilic wire mesh suppresses dry spots growth

and delays dryout, thereby postponing CHF.

ACKNOWLEDGEMENT

This work was supported by the Human Resources Development of the Korea Institute of Energy Technology Evaluation and Planning(KETEP) grant funded by the Ministry of Trade, Industry and Energy of Korea(No. RS-2023-00244330)

This work was supported by Korea Research Institute for defense Technology planning and advancement (KRIT) grant funded by the Korea government (DAPA (Defense Acquisition Program Administration)) (No. G08BR2200010101 (KRIT-CT-22-022), Ultra-High-Flux Cooling Systems Research Laboratory, 2022)

REFERENCES

[1] Rempe, Joy L., et al. "In-vessel retention of molten corium: lessons learned and outstanding issues." *Nuclear technology* 161.3 (2008): 210-267.
[2 Cheung, F. B. "Limiting factors for external reactor vessel cooling." *Nuclear technology* 152.2 (2005): 145-161.
[3] Park, Seong Dae, and In Cheol Bang. "Flow boiling CHF enhancement in an external reactor vessel cooling (ERVC) channel using graphene oxide nanofluid." *Nuclear Engineering and Design* 265 (2013): 310-318.
[4] Park, Seong Dae, and In Cheol Bang. "CHF enhancement through Pressurized Intermediate Layer in IVR-ERVC Strategy." *Transactions of the Korean Nuclear Society Spring Meeting. Jeju, Korea*. 2014.
[5] Song, Sub Lee, and Soon Heung Chang. "An experimental study on CHF enhancement of wire nets covered surface in R-134a flow boiling under high pressure and high mass flux conditions." *International Journal of Heat and Mass Transfer* 90 (2015): 761-768..
[6] Xie, Shangzhen, et al. "Review of critical-heat-flux enhancement methods." *International Journal of Heat and Mass Transfer* 122 (2018): 275-289.
[7] Kim, Hyungdae, et al. "Critical heat flux enhancement by single-layered metal wire mesh with micro and nano-sized pore structures." *International Journal of Heat and Mass Transfer* 115 (2017): 439-449.
[8] Park, Rae-Joon, Kwang-Soon Ha, and Hwan-Yeol Kim. "Detailed evaluation of natural circulation mass flow rate in the annular gap between the outer reactor vessel wall and insulation under IVR-ERVC." *Annals of Nuclear Energy* 89 (2016): 50-55.
[9] Jung, Jun Yeong, et al. "Flow boiling experiments for CHF evaluation under downward-facing heating including flow visualization: Effects of pressure, orientation, mass flux, and local quality." *Annals of Nuclear Energy* 171 (2022): 108994.
[10] Lee, C. H., and I. Mudawwar. "A mechanistic critical heat flux model for subcooled flow boiling based on local bulk flow conditions." *International Journal of Multiphase Flow* 14.6 (1988): 711-728.
[11] Kang, In Yeop, et al. "Effect of metallic wire-mesh on flow boiling CHF from the downward-facing heated wall." *Transactions of the Korean Nuclear Society Spring Meeting. Jeju, Korea*. 2022.